*Journal of Statistical Physics, Vol. 19, No. 1, 1978*

# Statistical Mechanics of a Nonlinear Stochastic Model

**Rashmi C. Desai**[1] **and Robert Zwanzig**[2]

*Received November 4, 1977*

A multivariable Fokker–Planck equation (FPE) is used to investigate the equilibrium and dynamical properties of a nonlinear stochastic model. The model displays a phase transition. The equilibrium distributions are found to be non-Gaussian; the deviation from Gaussian is especially significant near the transition point. To study the nonequilibrium behavior of the model, a self-consistent dynamic mean field (SCDMF) theory is derived and used to transform the FPE to a systematic hierarchy of equations for the cumulant moments of the time-dependent distribution function. These equations are numerically solved for a variety of initial conditions. During the time evolution of the system from an initial unstable equilibrium state to the final equilibrium state, three distinct time stages are found.

**KEY WORDS:** Fokker–Planck equation; cumulant moments; fluctuations far from equilibrium; nonlinear; Gaussian; non-Gaussian.

## 1. INTRODUCTION

In recent years, there has been a renewed interest in the study of fluctuations in nonlinear systems far from equilibrium. In this paper we present a study of the equilibrium and the dynamical properties of a specific nonlinear stochastic model, which displays many of the characteristics obtained by others[1-9] on general statistical mechanical grounds. In these articles, the techniques of Langevin equation,[1] Master equation,[2] and Fokker–Planck equation[3-7] have been used to study various aspects of the approach to equilibrium in nonlinear systems. Also, expansion in the inverse system size[1,2,8] has been used to investigate the most probable path during the time evolution and the deviations from it; specifically, an initial enhancement

Supported by a grant from the National Research Council of Canada (to RCD) and by the Sherman Fairchild Foundation (to RZ).

[1] Department of Physics, University of Toronto, Toronto, Ontario, Canada.

[2] Institute for Physical Science and Technology, University of Maryland, College Park, Maryland. Also Sherman Fairchild Distinguished Scholar, 1974–75, at the California Institute of Technology, where the early part of this research was done.



0022-4715/78/0700-0001$05.00/0 

of the variance has been predicted in many situations and the existence of various distinct time stages[7,9] has been found during the time evolution from an initial unstable state.

The nonlinear stochastic model that we have studied has been introduced recently by Kometani and Shimizu.[10] Below we give its detailed statement. To study its equilibrium and nonequilibrium properties, we use the multivariate Fokker–Planck equation (FPE). We discuss this as well as many of the equilibrium properties of the model in Section 2; we show that the model possesses a phase transition and find that the equilibrium distribution contains non-Gaussian characteristics, which are large, especially near the transition boundary in the parameter space of the model. In subsequent sections, we describe the behavior of the model system during the approach to equilibrium from various initial states.

In Section 3, we develop a self-consistent dynamic mean field (SCDMF) theory in two different but equivalent ways. From the FPE, one can derive a set of coupled equations satisfied by the reduced distribution functions $\rho_n$. The *first* way of obtaining the SCDMF theory is to truncate the hierarchy by replacing $\rho_2$ with $\rho_1\rho_1$. We then use the closed equation for $\rho_1$ to develop a hierarchy of equations for the *diagonal* cumulant moments of the full distribution function. The infinite hierarchy of equations are first-order, coupled, nonlinear differential equations and their structure can be cast in a form that is amenable to easy numerical integration. In the *second* way of obtaining the SCDMF theory, also discussed in Section 3, we start from the multivariate FPE, use cumulant moment expansion, and make a much weaker assumption that cross cumulants are *initially* $O(1/N)$. This results in the same hierarchy of equations for the *diagonal* cumulant moments.

In Section 4, we give the results of the numerical solution of these equations for a few interesting initial conditions and at various orders of truncation of the hierarchy. For all the cases studied, we find an initial enhancement of fluctuations. We also find three distinct time stages during the time evolution from an initial unstable state (class 3 of the initial conditions described in Section 4). We summarize the results in Section 5.

The nonlinear stochastic model of Kometani and Shimizu can be viewed as a system of $N$ anharmonic "oscillators." Each oscillator is described by the "coordinate" $a_i$, which obeys a stochastic equation of motion having the form of a multivariable nonlinear Langevin equation:

$$da_i/dt = v_i(a) + f_i, \qquad i = 1, 2, \ldots, N \tag{1}$$

where $\mathbf{a} \equiv \{a_1, a_2, \ldots, a_N\}$ and the stochastic force $f_i$ is assumed to be a Gaussian Markov process characterized by the diffusion constant $D$:

$$\overline{f_i} = 0 \tag{2a}$$

$$\overline{f_i(t_1)f_j(t_2)} = 2D\,\delta_{ij}\,\delta(t_1 - t_2), \qquad D > 0 \tag{2b}$$

with the bar over a quantity indicating the average over the Gaussian probability distribution of the stochastic force. The "velocity" of the $i$th oscillator is

$$v_i = pa_i - qa_i^3 + (\theta/N)\sum_j (a_j - a_i) \tag{3a}$$

where $q$ has to be positive in order to ensure stability; we shall also assume both $p$ and $\theta$ to be positive for simplicity. $v_i$ contains the linear and cubic single-particle terms and in addition contains the mean-field-like interaction term, which we shall refer to as the Weiss field since each oscillator interacts (constant interaction strength $\theta$) with *every other* oscillator in the system.

In the Langevin equation (1), $v_i$ represents the systematic force, which can also be viewed as derivable from a potential: $\mathbf{v} = -\partial\mathscr{H}/\partial\mathbf{a}$, where

$$\mathscr{H} = -\tfrac{1}{2}(p - \theta)\sum_j a_j^2 + \tfrac{1}{4}q\sum_j a_j^4 - (\theta/2N)\Big(\sum_j a_j\Big)^2 \tag{3b}$$

The single-particle terms would describe a potential well with a single minimum if $\theta > p$ and a double minimum if $\theta < p$. If $\theta < p$, then the minima occur at $a_j = \pm[(p - \theta)/q]^{1/2}$ and the depth of the well is $-(p - \theta)^2/4q$. Thus, if the strength of the nonlinear term $q$ is very small and $\theta < p$, then the wells are far apart and deep, indicating the localization of various oscillators. In the limit, one can see that the model in Eq. (3b) would reduce to the Ising–Weiss model. If, in addition, we let $N \to \infty$, the model given in Eqs. (1)–(3) can also be viewed as a model with space dimensionality one and spin dimensionality infinity. In this limit, the mean field approximation is known[11] to become exact. The analog of this feature in the time-dependent study can be seen in the equivalence of two descriptions of the SCDMF theory, as described above and in Section 3. One further point to note is that Eq. (3b) does not contain any "spatial" gradients; also, it does not refer to any underlying lattice. In this sense it is quite primitive compared to many of the models used in studying the equilibrium properties related to critical phenomena.

Even though the model contains four parameters, it is convenient, for the rest of this paper, to eliminate two of these ($p$ and $q$) through a simple scale transformation,

$$pt \to t' \qquad \text{and} \qquad (q/p)^{1/2}\mathbf{a} \to \mathbf{a}' \tag{4}$$

This transforms Eqs. (1)–(3) into a set of equations of the same form, except that $p$ and $q$ are replaced by unity, $D$ goes to $D' = Dq/p^2$, and $\theta$ goes to $\theta' = \theta/p$. Even though the transformation hides the strength of the linear and cubic terms in Eq. (1), it is clear that the model accomodates arbitrarily large nonlinearity. For ease of notation, we shall henceforth drop the primes on various symbols like $t'$, $\theta'$, $D'$, $\mathbf{a}'$, etc.

## 2. EQUILIBRIUM PROPERTIES

It can be shown that the nonlinear Langevin description of the model given in Section 1 is also equivalent to the Fokker–Planck equation (FPE) description for the noise-averaged probability distribution function of **a** at time $t$, $g(\mathbf{a}, t)$. The FPE equivalent to Eqs. (1)–(3) is

$$\frac{\partial}{\partial t} g(\mathbf{a}, t) + \sum_i \frac{\partial}{\partial a_i} [v_i(\mathbf{a}) g(\mathbf{a}, t)] = D \sum_i \frac{\partial^2}{\partial a_i^2} g(\mathbf{a}, t) \tag{5}$$

where it is convenient to write $v_i = -\partial \mathscr{H}(\mathbf{a})/\partial a_i$, with

$$\mathscr{H}(\mathbf{a}) = -\tfrac{1}{2}(1 - \theta) \sum_i a_i^2 + \tfrac{1}{4} \sum_i a_i^4 - (\theta/2N)\Big(\sum_j a_j\Big)^2 \tag{6}$$

The single-oscillator potential $\mathscr{H}_1(a_i)$

$$\mathscr{H}_1(a_i) = -\tfrac{1}{2}(1 - \theta) a_i^2 + \tfrac{1}{4} a_i^4 \tag{6a}$$

has a single minimum if the interaction strength $\theta > 1$ and a double minimum if $\theta < 1$. The FPE is a useful starting point to investigate various equilibrium and time-dependent properties of the model. Both Eqs. (1) and (5) are Markovian and the latter is linear in the distribution function $g(\mathbf{a}, t)$. It is well known that the equilibrium solution of Eq. (5) is

$$g_0(\mathbf{a}) = Q^{-1} \exp[-\mathscr{H}(\mathbf{a})/D] \tag{7a}$$

where

$$Q = \int d^N a \exp[-\mathscr{H}(\mathbf{a})/D] \tag{7b}$$

Even though the stochastic force **f** in Eq. (1) is Gaussian-distributed, the equilibrium distribution $g_0(\mathbf{a})$ is non-Gaussian, due to the nonlinear terms in Eq. (2). The diffusion constant $D$ is seen to be analogous to temperature.

The arithmetic mean of the oscillator coordinates $\sum_i a_i/N$ is a relevant dynamical variable for the model. Its average over the noise source **f** and the probability distribution $g(\mathbf{a}, t)$ will be denoted by $x(t)$; $x$ plays the role of the order parameter for the model and is defined to be an intensive variable.

One can also deduce from $g_0(\mathbf{a})$ the equilibrium probability distribution for the order parameter $x$,

$$P_0(x) = \left\langle \delta\Big(\sum_i a_i/N - x\Big) \right\rangle_0 \tag{8a}$$

$$\equiv \int d^N a \, \delta\Big(\sum_i a_i/N - x\Big) g_0(\mathbf{a}) \tag{8b}$$

in the limit of large $N$, using the saddle-point method and the integral

representation of the delta-function. This asymptotic result would be the leading term in the system size expansion of $P_0(x)$. The result is

$$P_0(x) \sim Q^{-1}\left[\frac{N}{2\pi\psi''(\bar{\omega})}\right]^{1/2} \exp\left\{N\left[\frac{\theta}{2D}x^2 - \bar{\omega}x + \psi(\bar{\omega})\right]\right\} \tag{9a}$$

where

$$\exp\psi(\omega) = \int_{-\infty}^{\infty} da \exp\{\omega a - [\tfrac{1}{2}(\theta - 1)a^2 + \tfrac{1}{4}a^4]/D\} \tag{9b}$$

and $\bar{\omega}$ is the saddle point, which depends on $x$ and is to be determined from the relation

$$x = [d\psi(\omega)/d\omega]_{\omega=\bar{\omega}} \tag{10}$$

The quantity $\psi(\omega)$ is related to $\mathscr{H}_1(a_i)$, Eq. (6a). We have not been able to evaluate the integral in Eq. (9b) in closed form, but the result can be written as an infinite series sum:

$$\exp\psi(\omega) = (2D)^{1/4}\sqrt{\pi}\sum_{n=0}^{\infty}\frac{1}{n!}\left(\frac{\omega^2\sqrt{D}}{2\sqrt{2}}\right)^n\left(\exp\frac{z^2}{4}\right)D_{-n-1/2}(z) \tag{11a}$$

$$\equiv [\exp\psi(0)]\sum_{n=0}^{\infty}A_n\omega^{2n}/n! \tag{11b}$$

where $z = (\theta - 1)/(2D)^{1/2}$ and $D_{-n-1/2}(z)$ is related to the parabolic cylinder functions.[3] The qualitative difference in $\mathscr{H}_1$ for $\theta > 1$ and $\theta < 1$ manifests itself through different functional behavior of $D_{-n-1/2}(z)$ for positive and negative values of $z$. Further inspection of Eqs. (9a) and (11) also reveals that $P_0(x)$ is non-Gaussian in character. Its origin appears to be in the quartic term in $\mathscr{H}_1$ rather than the interaction term in $\mathscr{H}$, since the distribution remains non-Gaussian when the limit $\theta \to 0$ is taken in the final result. In the limit of large $z$ (this includes the limit of small $D$, which implies a neglect of the stochastic-force-related fluctuations), $P_0(x)$ approaches a Gaussian, however.

The value of the order parameter $x$ in equilibrium is $x_0 \equiv \int dx\, xP_0(x)$; for large $N$, it would also be equal to the most probable value $\bar{x}$: $dP_0(\bar{x})/d\bar{x} = 0$. From Eq. (9a), we find

$$\bar{x} = x_0 = (D/\theta)\omega_0 \tag{12a}$$

Also, this value of $x$ must satisfy Eq. (10), which implies

$$x_0 = \left[\frac{d\psi(\omega)}{d\omega}\right]_{\omega=\omega_0} = \frac{\int_{-\infty}^{\infty} da\, ae^{\omega_0 a}e^{-\mathscr{H}_1(a)/D}}{\int_{-\infty}^{\infty} da\, e^{\omega_0 a}e^{-\mathscr{H}_1(a)/D}} \tag{12b}$$

[3] See Fig. 2 of Ref. 13 and the relevant discussion in the text.

These two equations together determine the order parameter $x_0$ as a function of the model parameters $D$ and $\theta$. A study of this functional dependence shows that there are two regions in the $(D, \theta)$ space: one in which the model system is in disordered phase with $x_0 = 0$ ($z < z_c$; $\theta > \theta_c$ for $\theta > 1$, $\theta < \theta_c$ for $\theta < 1$), and the second region, which corresponds to an ordered phase. In this phase, for every value of $z > z_c$, there are three possible steady-state values of $x$: zero, which is unstable, and $\pm x_0$. The boundary between the two phases can be found from Eqs. (11) and (12) and is determined via a relation that the parameters $(D_c, \theta_c)$ must satisfy. This relation is

$$\frac{(2D_c)^{1/2}}{\theta_c} = \frac{\theta_c - 1}{z_c\theta_c} = \frac{D_{-3/2}(z_c)}{D_{-1/2}(z_c)} \tag{13}$$

The solid line in Fig. 1 shows the solution[14] of this transcendental equation; $\theta_c < 1$ corresponds to the double minimum in the single-oscillator Hamiltonian $\mathscr{H}_1$, and $\theta_c > 1$ to the single minimum. If we approximate[10] $\exp \psi(\omega)$ in Eq. (11) by a Gaussian, the approximate relation between the model parameters is $\theta_c = 3D_c$. The result of the Gaussian approximation is shown as a dashed line in Fig. 1. Significant difference is found between the exact and the approximate results.

In the ordered phase, one can also inquire about the behavior of the

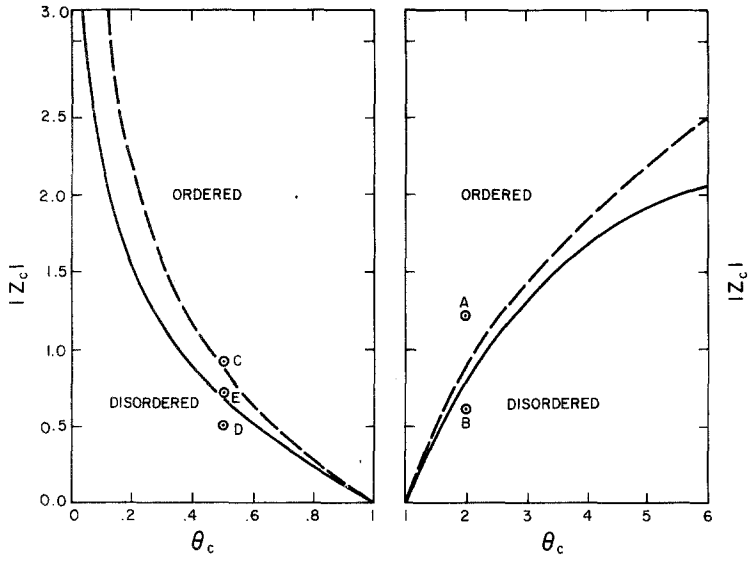


Fig. 1. The boundary between the ordered and disordered phases in the model parameter space: solid line, solution of exact Eq. (13); dashed line, Gaussian approximation.

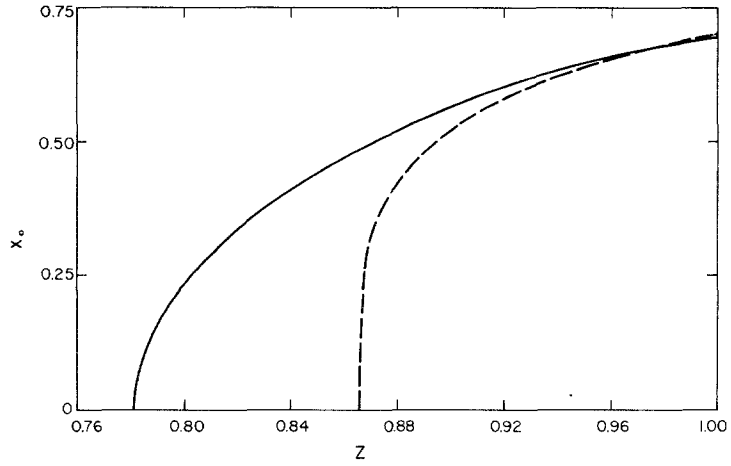


Fig. 2. The equilibrium order parameter $x_0$ as a function of $z = (\theta - 1)/(2D)^{1/2}$ for $\theta = 2$. Solid line, exact result; dashed line, Gaussian approximation, Eq. (14).

order parameter as a function of $D$ and $\theta$. This query can be answered analytically in the Gaussian approximation[10] and one gets

$$x_0 = \pm\{(2 - \theta) + [(2 + \theta)^2 - 24D]^{1/2}\}^{1/2}/2 \tag{14}$$

The exact result for $x_0$, however, can only be obtained numerically through Eqs. (11) and (12). In Fig. 2 we show the comparison of the two results for $\theta = 2$. It is interesting and useful to know that the Gaussian approximation becomes quite good away from the bifurcation point $z_c$.

The behavior of $x_0$ in the neighborhood of $z_c$ is mean-field-like: For a fixed $\theta$, if one decreases $D$ in the neighborhood of $D_c$, the order parameter varies as

$$x_0 = [3(\theta_c - 1)/2\theta_c^2]^{1/2}(D_c - D)^{1/2} \tag{15}$$

From the nature of the interaction term in Eq. (3), the mean-field-like behavior is expected. From Eqs. (11) and (12), one can also write

$$z = z_c + m_1\omega_0^2 + m_2\omega_0^4 + \cdots \tag{16a}$$

with

$$m_1 = \sqrt{D_c}/3\sqrt{2}$$

and

$$m_2 = -\frac{(2D_c)^{1/2}}{180}\frac{1 - \theta_c + 3D_c - 5D_c/\theta_c}{1 - 3D_c/\theta_c} \tag{16b}$$

Thus, due to Eqs. (12a) and (16), the curvature of $x_0(z)$ in the neighborhood

of the bifurcation point is known analytically. Finally, let us note that in the model system studied in this paper, the bifurcation point and the transition point are the same. One can of course construct other models where these two need not occur at the same point in the parameter space.

## 3. SCDMF AND CUMULANT MOMENTS

In this section, we use the FPE, Eq. (5), to study the dynamical properties of the stochastic model. We develop a self-consistent dynamic mean field (SCDMF) theory in two ways and find that they are equivalent. In the first way, we obtain an equation that the singlet distribution $\rho(a_1, t)$ satisfies. Then we derive a hierarchy of equations that various cumulant moments of $\rho(a_1, t)$ obey. In the second method, we show that the same hierarchy can also be obtained directly from the FPE via a somewhat weaker assumption. Finally, we discuss the equilibrium solutions of the hierarchy for various model parameters; Section 4 contains the time-dependent solutions for various initial conditions.

In the time evolution study, one important point needs to be made first. For purely dynamical systems, it is known that the time evolution can be studied in a formally equivalent way by following either the distribution function or the dynamical variable of interest. The same is true for the stochastic models: If we formally write Eq. (5) as

$$\partial g(\mathbf{a}, t)/\partial t = \mathscr{D} g(\mathbf{a}, t) \tag{17a}$$

to define the Fokker–Planck operator $\mathscr{D}$, and use

$$\int d^N a\, A(\mathbf{a}) \mathscr{D} g(\mathbf{a}) = \int d^N a\, \{\mathscr{D}^+ A(\mathbf{a})\} g(\mathbf{a}) \tag{17b}$$

to construct the adjoint operator $\mathscr{D}^+$, then we can show that

$$\int d^N a\, A[\mathbf{a}(t)] g(\mathbf{a}, 0) = \int d^N a\, A(\mathbf{a}) g(\mathbf{a}, t) \tag{17c}$$

where

$$\mathbf{a}(t) = [\exp(\mathscr{D}^+ t)]\mathbf{a} \tag{17d}$$

Thus the average of the dynamical variable $A$ over the time-dependent distribution $g(\mathbf{a}, t)$ is equivalent to that of $A[\mathbf{a}(t)]$ over the initial ensemble, the noise average implied in both cases.

The time evolution for the stochastic model can be studied at various levels of approximation. An interesting way is to proceed via the hierarchy of equations satisfied by the reduced distribution functions. Let us define

$$\rho_s(a_1, \ldots, a_s, t) = \int da_{s+1} \cdots da_N\, g(\mathbf{a}, t) \tag{18}$$

Starting from the FPE, Eq. (5), it is easy to derive the hierarchy satisfied by $\rho_s$. A simple way to truncate it is to make an ansatz that generates the self-consistent dynamic mean field (SCDMF) result:

$$\rho_2(a_1, a_2, t) \approx \rho(a_1, t)\rho(a_2, t) \tag{19}$$

With this ansatz, the singlet distribution $\rho(a_1, t)$ of the stochastic model satisfies the following equation as $N \to \infty$:

$$\frac{\partial \rho}{\partial t} + \frac{\partial}{\partial a_1}\{[\theta x(t) - (\theta - 1)a_1 - a_1{}^3]\rho\} = D\frac{\partial^2 \rho}{\partial a_1{}^2} \tag{20a}$$

where

$$x(t) = \int_{-\infty}^{\infty} da_1\, a_1 \rho(a_1, t) \tag{20b}$$

Since the time-dependent order parameter $x(t)$ appears in Eq. (20), it is appropriate to call Eq. (19) a self-consistent ansatz. The cumulant moments $M_n(t)$ of the singlet distribution $\rho(a_1, t)$ are determined from the coefficients of $\alpha^n$ in the $\alpha$ expansion of $\ln F(\alpha, t)$, where

$$F(\alpha, t) = \int_{-\infty}^{\infty} da_1\, \rho(a_1, t) e^{\alpha a_1} \tag{21}$$

$x(t)$ is clearly synonymous with the first cumulant moment $M_1(t)$. When we use Eq. (20) to deduce the equation of motion for the generating function $F(\alpha, t)$ and collect the $\alpha^n$ coefficients in the Taylor series expansion, we get

$$\begin{aligned}\frac{1}{n}\frac{dM_n(t)}{dt} &= D\delta_{n2} + \theta M_1(t)\,\delta_{n1} - (\theta - 1)M_n(t) \\ &\quad - M_{n+2}(t) - 3\sum_{i=1}^{n} \frac{(n-1)!}{(i-1)!\,(n-i)!} M_i(t) M_{n-i+2}(t) \\ &\quad - \sum_{i=1}^{n}\sum_{j=1}^{n-i+1} \frac{(n-1)!}{(i-1)!\,(j-1)!\,(n-i-j+1)!} \\ &\quad \times M_i(t) M_j(t) M_{n-i-j+2}(t)\end{aligned} \tag{22}$$

These are an infinite hierarchy of first-order, coupled, nonlinear differential equations. The cumulant moment $M_n$ couples to all the moments $M_k$ with $k \leqslant n + 2$, due to the cubic nonlinearity in the "velocity" of the stochastic model. Since such differential equations occur in many areas of statistical physics, efficient numerical techniques to solve them (with a finite-order truncation) are available. The method we use is indicated in Section 4. The

structure of Eq. (22) can also be reorganized for fast computation by rewriting the last two terms. The equivalent form of these two terms that we have used to generate the numerical solutions for $M_n(t)$ is

$$-\Bigg\{3M_1M_{n+1} + 3\sum_{k=1}^{[n/2]}\binom{n}{k}'M_{k+1}M_{n-k+1} + (n-1)!\sum_{i=1}^{[(n+2)/3]}\frac{M_i}{(i-1)!} \times \sum_{j=i}^{[(n+2-i)/2]}\frac{M_jM_{n-i-j+2}}{(j-1)!\,(n-i-j+1)!}\,C_{i-1,j-1}^{n-i-j+1} \tag{23a}$$

where $[l]$ indicates the integral part of $l$,

$$\begin{aligned}\binom{n}{k}' &= \frac{n!}{k!\,(n-k)!} && \text{unless } k = \left[\frac{n}{2}\right] \text{ and } n \text{ is even}\\ &= \frac{1}{2}\frac{n!}{k!\,(n-k)!} && \text{if } k = \left[\frac{n}{2}\right] \text{ and } n \text{ is even}\end{aligned} \tag{23b}$$

and

$$\begin{aligned}C_{l,m}^{n} &= 1 && \text{if } l, m, n \text{ are equal}\\ &= 3 && \text{if any two of } l, m, n \text{ are equal}\\ &= 6 && \text{if } l, m, n \text{ are distinct}\end{aligned} \tag{23c}$$

Even though Eq. (22) for the cumulant moments has been obtained via the truncation ansatz Eq. (19), we have found an alternate approach, which also leads to Eq. (22). In this approach, we begin with the FPE, Eq. (5), and deduce the equation of motion for a more detailed generating function $\mathscr{F}(\gamma, t)$,

$$\mathscr{F}(\gamma, t) = \left\langle \exp\Big(\sum_i \gamma_i\xi_i\Big); \mathbf{a}\right\rangle_{\text{ne}} \tag{24a}$$

$$\equiv \int d^Na\left[\exp\Big(\sum_i \gamma_i\xi_i\Big)\right]g(\mathbf{a}, t) \tag{24b}$$

where $\xi_i$ are the fluctuation of $a_i$ about the most probable path $x(t) \equiv \int d^Na\, a_ig(\mathbf{a}, t)$, i.e., $\xi_i = [a_i - x(t)]$. For simplicity, we assume all the oscillators to be statistically equivalent and first derive the equation of motion for $\mathscr{F}(\gamma, t)$ from the FPE. We find

$$\frac{\partial\mathscr{F}}{\partial t} = \sum_i \gamma_i\Big[x - x^3 - \frac{dx}{dt} + \gamma_iD + (1 - 3x^2)\frac{\partial}{\partial\gamma_i} - 3x\frac{\partial^2}{\partial\gamma_i^2} - \frac{\partial^3}{\partial\gamma_i^3} + \frac{\theta}{N}\sum_m\Big(\frac{\partial}{\partial\gamma_m} - \frac{\partial}{\partial\gamma_i}\Big)\Big]\mathscr{F} \tag{25}$$

We now substitute in Eq. (25) the expansion

$$\mathscr{F}(\boldsymbol{\gamma}, t) = 1 + \sum_i \gamma_i \mathscr{F}_i(t) + \sum_i \sum_j \frac{1}{2!} \gamma_i \gamma_j \mathscr{F}_{ij}(t) + \sum_i \sum_j \sum_k \frac{1}{3!} \gamma_i \gamma_j \gamma_k \mathscr{F}_{ijk}(t) + \cdots \tag{26}$$

where $\mathscr{F}_{ij} = (\partial^2 \mathscr{F}/\partial\gamma_i\, \partial\gamma_j)_{\gamma=0}$, etc., and equate various coefficients of powers of $\boldsymbol{\gamma}$ to get the expressions for various derivatives of $\mathscr{F}$ with respect to $\boldsymbol{\gamma}$ at $\boldsymbol{\gamma} = 0$. We note from Eq. (24) that

$$\mathscr{F}_i = \langle \xi_i; \mathbf{a} \rangle_{\text{ne}} = \langle a_i; \mathbf{a} \rangle_{\text{ne}} - x(t) \tag{27}$$

which is zero by definition of $x(t)$. Using this result, the equation of motion for $x(t)$ is obtained by equating the coefficients of the linear term in $\boldsymbol{\gamma}$. Higher order derivatives of $\mathscr{F}(\boldsymbol{\gamma}, t)$ can be related to the cumulant moments of $g(\mathbf{a}, t)$ by considering the $\boldsymbol{\gamma}$ expansion of $\ln \mathscr{F}(\boldsymbol{\gamma}, t)$. One gets

$$\begin{aligned} \mu_{ij}(t) &\equiv \langle \xi_i \xi_j; t \rangle_{\text{ne}}^{c} = \mathscr{F}_{ij}(t) \\ \mu_{ijk}(t) &\equiv \langle \xi_i \xi_j \xi_k; t \rangle_{\text{ne}}^{c} = \mathscr{F}_{ijk}(t) \\ \mu_{ijkl}(t) &\equiv \langle \xi_i \xi_j \xi_k \xi_l; t \rangle_{\text{ne}}^{c} = \mathscr{F}_{ijkl}(t) - 3\mathscr{F}_{ij}(t)\mathscr{F}_{kl}(t) \end{aligned} \tag{28}$$

etc., where statistical equivalence of different oscillators is used. The cumulant moments fall into two categories: The first one consists of the diagonal moments for which $i = j = k = \cdots$; we shall denote these by $M_n(t)$, which is the cumulant moment of $\xi_i^n$; e.g., $\mu_{iii}(t) \equiv M_3(t)$. The rest of the moments are the cross cumulant moments. The statistical equivalence of the oscillators implies that the cumulant moments for the first four orders will be $x(t)$; $M_2(t)$, $\mu_{12}(t)$; $M_3(t)$, $\mu_{112}(t)$, $\mu_{123}(t)$; and $M_4(t)$, $\mu_{1112}(t)$, $\mu_{1122}(t)$, $\mu_{1123}(t)$ and $\mu_{1234}(t)$.

In the appendix we give the coupled equations of motion for these 11 cumulant moments, which are obtained by neglecting fifth- and higher-order cumulant moments. From these equations, we can see that the role of diagonal and cross cumulant moments in the hierarchy of coupled equations is different. In particular, if we restrict our discussion to those initial ensembles in which all the cross cumulant moments are at least $O(1/N)$ at $t = 0$, then their equations of motion lead to the conclusion that they remain $O(1/N)$ at all later times [see Eqs. (A3), (A5), (A6), and (A8)–(A11)]. Thus we approximate the moment equations by taking the large-$N$ limit (i.e., retain the leading term in the inverse system size expansion); this reduces the equations for the diagonal cumulant moments $M_n(t)$ to the hierarchy given in Eq. (22).

It is interesting that even though Eq. (19) is a much stronger approximation compared to the one that retains the leading terms in the inverse system size expansion, the cumulant moments follow identical time evolution. The equivalence of the results obtained by these two methods is the dynamic

analog of the known[11] property of the Ising–Weiss model in equilibrium that the mean field results become exact in the limit $N \to \infty$. Thus we refer to the two schemes leading to Eq. (22) as the SCDMF theory. We have used the cumulant moment equations (22) to (a) find the equilibrium solutions $M_n(\infty)$ for various parameter $(D, \theta)$ values, (b) study time evolution for interesting initial conditions, and (c) study various approximations for their solution.

The equilibrium moments $M_{n0}$ can, in principle, be directly obtained from the equilibrium distribution discussed in Section 2, since $g(\mathbf{a}, \infty) \equiv g_0(\mathbf{a})$. Specifically, since these are cumulant moments related to the fluctuation $\xi_i = a_i - x_0$, the generating function is

$$\mathscr{F}_0(\gamma, t) = \int d^N a \exp\Big(\sum_i \gamma_i \xi_i\Big)\, \delta\Big(\sum_i a_i/N - x\Big)\, g_0(\mathbf{a}) \Big/ P_0(x) \tag{29a}$$

$$\equiv \left\langle \exp\Big(\sum_i \gamma_i \xi_i\Big) ; \mathbf{a} \right\rangle_0 \tag{29b}$$

where $g_0(\mathbf{a})$ and $P_0(x)$ are as defined in Eqs. (7) and (8). The integrals involved in evaluating the equilibrium moments $M_{n0}$ can be approximately obtained via the saddle-point method. We find that in terms of $\bar{\omega}$ and $A_n$ defined in Eqs. (9c) and (11),

$$x_0 \equiv \langle a_i ; \mathbf{a} \rangle_0 = [2A_1\bar{\omega} + 2(A_2 - A_1{}^2)\bar{\omega}^3 + (A_3 - 3A_1A_2 + 2A_1{}^3)\bar{\omega}^5 + (\tfrac{1}{3}A_4 - A_2{}^2 + \tfrac{4}{3}A_1A_3 + 4A_1{}^2A_2 - 2A_1{}^4)\bar{\omega}^7 + \cdots]_{\bar{\omega}=\omega_0} \tag{30a}$$

$$M_{20} = (dx_0/d\bar{\omega})_{\bar{\omega}=\omega_0} \tag{30b}$$

$$M_{30} = (d^2x_0/d\bar{\omega}^2)_{\bar{\omega}=\omega_0} \tag{30c}$$

and

$$M_{40} = [d^3x_0/d\bar{\omega}^3 + 3(dx_0/d\bar{\omega})^2]_{\bar{\omega}=\omega_0} \tag{30d}$$

Since these results are expressed in powers of $\bar{\omega}$, they are useful only close to the bifurcation point. Far from it, the Gaussian approximation is adequate. In the intermediate region of the parameter space, the equilibrium moments can be obtained from the steady-state limiting values at long times in the numerical solution of Eq. (22). As an example, the equation of motion for $x(t)$ is, from Eq. (22),

$$dx/dt = x - x^3 - 3xM_2 - M_3 \tag{31a}$$

In steady state, $dx/dt$ vanishes and we can use Eqs. (30b) and (30c) to get

$$0 = x_0 - x_0{}^3 - 3x_0 \frac{dx_0}{d\omega_0} - \frac{d^2x_0}{d\omega_0{}^2} \tag{31b}$$

which in turn reduces to, using Eq. (30a),

$$(A_1 - 6A_2) + \omega_0{}^2(A_2 - A_1{}^2 + 6A_1A_2 - 10A_3) + \cdots = 0 \tag{31c}$$

Thus the parameters $(D_c, \theta_c)$ at the bifurcation point (Section 2, Fig. 1) will satisfy the relation

$$A_1 = 6A_2 \tag{32}$$

If we use the definition of $A_n$, Eq. (11), this relation reduces to Eq. (13), indicating the internal consistency. In order to find the equilibrium values of various cumulant moments in the region of the $(D, \theta)$ space away from the bifurcation point (but not so far away that the Gaussian approximation is good), we solve Eq. (22) numerically (see Section 4) by truncating the hierarchy at various orders. The convergence of the results is quite rapid for low-order moments: For ordered states, both $x_0$ and $M_{20}$ obtained by setting $M_n = 0$ for $n > 5$ are found correct to four significant figures; for $M_{30}$ this is found with $n > 7$, and for $M_{40}$ with $n > 10$; for disordered states all odd moments vanish and the convergence of the even moments to similar degree of accuracy requires the same number of equations, i.e., four-figure accuracy in $M_{20}$ requires truncation at $n > 10$. In Fig. 3, we show the behavior of $M_{20}$ as a function of $z$ obtained from the numerical solution of Eq. (24) with $\theta = 2$ and varying $D$. We find that $M_{20}$ decreases monotonically with $z$. In Gaussian approximation, $M_{20}$ can be obtained analytically; it is

$$\begin{aligned} M_{20} &= \{2 + \theta - [(2 + \theta)^2 - 24D]^{1/2}\}/12, && \text{ordered phase} \\ &= 1/3, && \text{at the bifurcation point} \\ &= \{1 - \theta + [(1 - \theta)^2 + 12D]^{1/2}\}/6, && \text{disordered phase} \end{aligned} \tag{33}$$

This is also shown for comparison (as dashed line) in Fig. 3. Equation (33) shows that the behavior of $M_{20}$ is analytically different on the two sides of

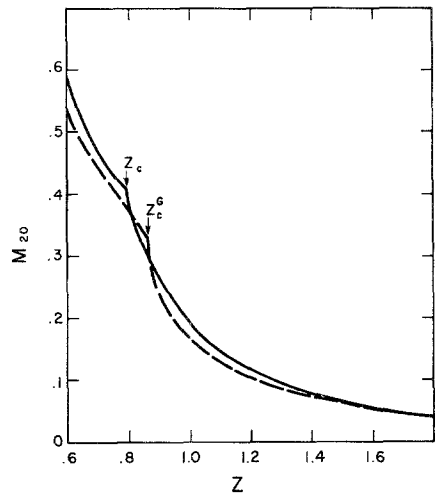


Fig. 3. The equilibrium second cumulant moment $M_{20}$ as a function of $z = (\theta - 1)/(2D)^{1/2}$ for $\theta = 2$. Solid line, exact result; dashed line, Gaussian approximation, Eq. (33).

the Gaussian bifurcation point (for Fig. 3, $\theta_c = 2$, $D_c = 2/3$, $Z_c = \sqrt{0.75} = 0.866$). Similar anomalous behavior is also apparent in the exact numerical data around the true bifurcation point ($Z_c = 0.782$).

## 4. TIME EVOLUTION

In this section we give the results of the numerical solution of the cumulant moment equations (22). For the time evolution studies away from the bifurcation point, we have used a FORTRAN program MODDEQ, which solves a system of first-order differential equations (not exceeding 20) and which uses the Runge–Kutta–Gill method of integration in conjunction with the Adams–Moulton predictor–corrector formulas. Close to the bifurcation point, Eq. (22) become stiff and we follow a different numerical procedure as developed by Gear and subsequently modified by Enright.[14] For all the results reported here, the convergence of the solution of Eq. (22) at various orders of truncation of the hierarchy is rapid and one gets quantitatively the same results for truncation at $n \geqslant 6$.

We have studied the approach to equilibrium for three different classes of initial conditions:

(i) At time $t = 0^-$, the system is in an equilibrium ordered state $[M_n(0^-) = M_{n0}]$; at that time the value of the order parameter is reduced by a factor of ten $[x(0^+) \equiv M_1(0^+) \approx 0.1x_0]$, leaving the rest of the cumulant moments unchanged. This class of initial conditions can be used to study the behavior of the most probable path and the fluctuations around it for nonlinear systems *far* from equilibrium.

(ii) At $t = 0^-$, the system is in an equilibrium *ordered* state; at that time one of the two model parameters ($D$, $\theta$) is changed such that the new equilibrium would correspond to a *disordered* state (see, for example, Fig. 1). The time evolution would then be analogous to the situation for the first-order phase transition as in *melting*. If, for example, $D$ is fixed and $\theta$ is changed from a value less than one to greater than one, then it is clear from Eq. (6b) that the double-well potential is changed to a single-well one at $t = 0^+$. This is one of the possible initial conditions in this class.

(iii) This class is the reverse of class (ii). At $t = 0^-$, the system is in an equilibrium *disordered* state with $x(0^-)$ and all odd moments zero; at that time one of the parameters (either $D$ or $\theta$) is altered to correspond to a new equilibrium ordered state. Now at $t = 0^+$ the system is in the metastable state with two possible directions ($\pm x_0$) to go to; we make that choice by simultaneously changing $x(0^-) = 0$ to $x(0^+) = +x_0/1000$. This is not a thermodynamic fluctuation, since Eq. (22) already corresponds to infinite ($N \to \infty$) number of oscillators in the system; it has to be perceived as a thermodynamically large, externally induced perturbation. Since there has

Table I. Equilibrium Cumulant Moments for Various States A–E

| | A Ordered | B Disordered | C Ordered | D Disordered | E Ordered |
|---|---|---|---|---|---|
| $D$ | 1/3 | 4/3 | 0.15 | 0.5 | 0.25 |
| $\theta$ | 2 | 2 | 1/2 | 1/2 | 1/2 |
| $\|z\|$ | 1.22 | 0.61 | 0.91 | 0.5 | 0.71 |
| $x_0$ | 0.8327 | 0 | 0.7980 | 0 | 0.1388 |
| $M_{20}$ | 0.1091 | 0.5623 | 0.1497 | 0.5842 | 0.4497 |
| $M_{30}$ | −0.0173 | 0 | −0.0687 | 0 | −0.0511 |
| $M_{40}$ | 0.0048 | −0.1774 | 0.0360 | −0.2318 | −0.1365 |
| $M_{50}$ | −0.0010 | 0 | −0.0040 | 0 | 0.0726 |

been considerable recent interest in the behavior of $x(t)$ and the associated anomalous fluctuations near unstable equilibrium,[2,4–7] and since it has also been found that linearization around the unstable state is unsatisfactory,[7] this class of initial states is of great interest for our numerical study.

In Table I, we give the equilibrium values of the cumulant moments $M_{n0}$ for five different states (three ordered—A, C, E—and two disordered—B, D), which we have used in the time evolution study. They are also shown in Fig. 1, which gives their position relative to the phase separation curve in the parameter space. For $\theta_c = 2$ we find $D_c = 0.8124$ and $z_c = 0.7845$, and for $\theta_c = 1/2$ we find $D_c = 0.264$ and $|z_c| = 0.688$. The location of state E is chosen such that it is an ordered state but the Gaussian approximation assigns to it a disordered state.

Initial conditions of class (i) described above were used for states A, C, and E. In Fig. 4, we show the results for the evolution of $x(t)$, $M_2(t)$, and $M_3(t)$ for state A. For the other two states the qualitative behavior of $x$ and $M_2$ was found to be similar, but the time scale over which the equilibrium was restored became larger (critical slowing down) for states closer to the bifurcation point. (Compared to the state A shown in Fig. 4, the comparable time span for state E was about 25 times larger.) The enhancement of $M_2$ at short times also occurred in all three cases, but for state E, it was quite small [$M_2(0) = M_2(250) \simeq 0.45$; $M_2(3) = 0.456$]. The behavior of $M_3(t)$ was similar for states A and C, but for state E, it had only the maximum and the secondary minimum was absent.

In Fig. 4, we also show (as dashed line) the result for $x(t)$ and $M_2(t)$ if Eq. (22) is truncated by setting $M_n(t) = 0$ for $n \geqslant 3$. Such a Gaussian approximation leads to quite a good result for the time evolution, since state A is far from the bifurcation point. Higher-order truncation leads to rapid convergence. Another approximation (#1, Section 4, Ref. 6) that has been

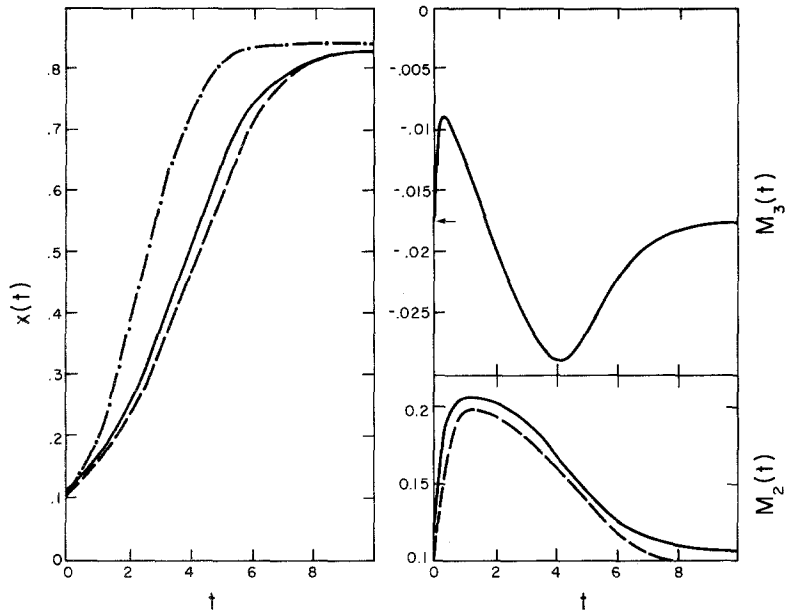


Fig. 4. $x(t)$, $M_2(t)$, and $M_3(t)$ for the first class of initial condition with $x(0) = 0.1$; $x_0$, $M_{20}$, $M_{30}$ for state A. Solid line, exact evolution; dashed line, Gaussian approximation; dot-dashed line, Eq. (34).

suggested would set $M_n(t) = 0$ for $n \geqslant 3$ and ignore the time variation in $M_2(t)$, i.e., $M_2(t) = M_{20}$. This leads to the result

$$x(t) = x(0)x_0\{[x(0)]^2 + \{x_0^2 - [x(0)]^2\} \exp(-2x_0^2 t)\}^{-1/2} \tag{34}$$

This is also shown in Fig. 4. The approach to the equilibrium value $x_0$ is somewhat faster in this approximation.

Initial conditions of class (ii) correspond to a situation in which the system is constrained to be in an ordered state at $t = 0^-$, the constraint is removed at $t = 0^+$, and the evolution toward the final equilibrium disordered state occurs. We have solved Eq. (22) for the two cases: one in which state A evolves toward state B, and another where state E evolves toward state D. The results for $x(t)$ and $M_2(t)$ are shown in Fig. 5 for the A $\rightarrow$ B evolution. $M_3(t)$ and $M_4(t)$ also show similar monotonic change from initial to final values. The qualitative behavior is identical for the E $\rightarrow$ D evolution. Also, the time scale on which the equilibrium is approached is the same in the two cases: By $t = 10$, equilibrium is achieved to three significant figures. Qualitatively, the time evolution here is analogous to the following situation (see Fig. 6). At $t = 0^-$, the probability distribution $\rho(a, t)$ is at the position of the minimum in the constrained double-well potential (shown by the arrow); at

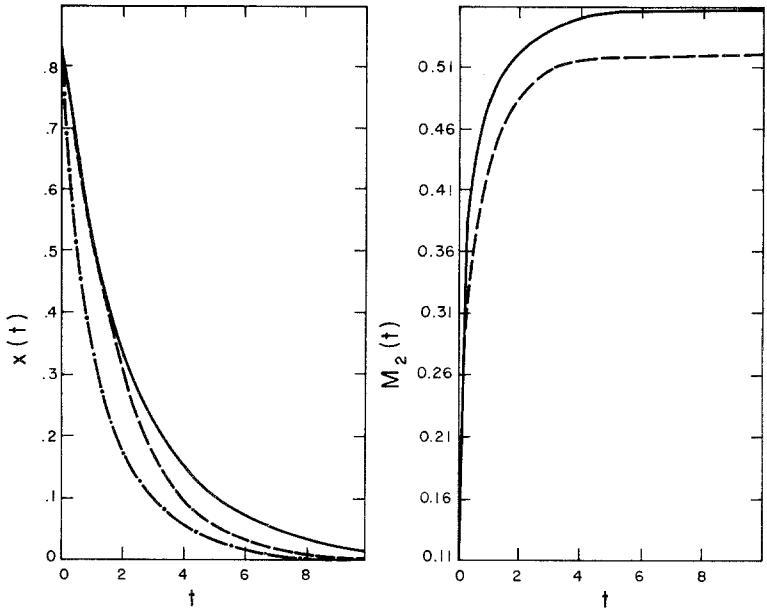


Fig. 5. $x(t)$ and $M_2(t)$ for the order → disorder transition corresponding to state A → state B. Solid line, exact evolution; dashed line, Gaussian approximation; dot-dashed line, Eq. (34).

$t = 0^+$, the constraint is removed, the well is now transformed to one with a single minimum, and the distribution falls. Clearly the decay would be monotonic and the time scale for approach to equilibrium is determined by the final state.

In Fig. 5, we also show the result of the truncation that sets $M_n = 0$ for $n \geqslant 3$, as a dashed line. The convergence of the sequential truncation at

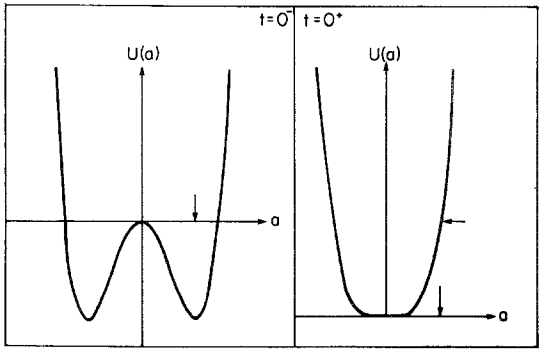


Fig. 6. Qualitative picture of the initial condition for order → disorder evolution.

$n = 4, 5, 6$ is rapid; $x(t)$ at successive order straddles the exact curve and the result at $n = 6$ coincides almost exactly with the exact result; $M_2(t)$ approaches the exact curve from below as truncation order is increased, with convergence achieved at $n = 6$. In Fig. 5, we also show the result for the approximation that led to Eq. (34) for the class (i) type of initial conditions. Here also one can obtain the analytic result for $x(t)$,

$$x(t) = ax(0)\{(a^2 + [x(0)]^2)\exp(2a^2t) - [x(0)]^2\}^{-1/2} \tag{35a}$$

where

$$a = (3M_{20} - 1)^{1/2} \tag{35b}$$

Again we find that the consequence of the neglect of the time variation in $M_2(t)$ and higher orders is to render the approach to equilibrium faster. In terms of the qualitative picture above, the entire distribution $\rho(a, t)$ falls coherently with no time lost in the spreading out of the distribution.

The final class of initial conditions gives rise to the most interesting time evolution. This is the reverse of the class (ii) initial conditions; it corresponds to the disorder-to-order evolution and may mimic a first-order phase change corresponding to freezing. We have solved Eq. (22) for the two cases: state B $\rightarrow$ state A and state D $\rightarrow$ state C. In Fig. 7 we show the evolution of $x(t)$ and $M_3(t)$ and in Fig. 8 the evolution of $M_2(t)$ and $M_4(t)$ for the

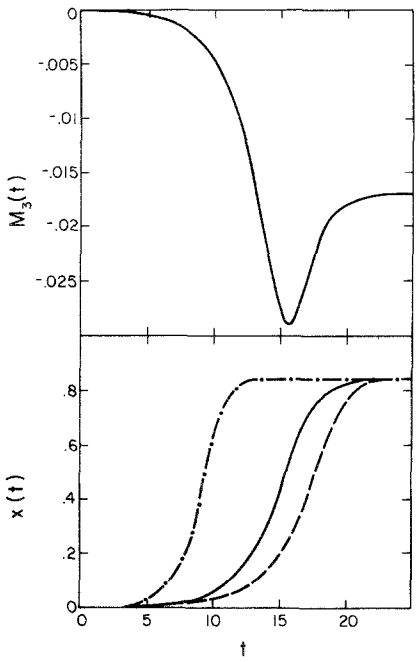


Fig. 7. $x(t)$ and $M_3(t)$ during the time evolution from an unstable to stable equilibrium. Solid line, exact; dashed line, Gaussian approximation; dot-dashed line, Eq. (34).

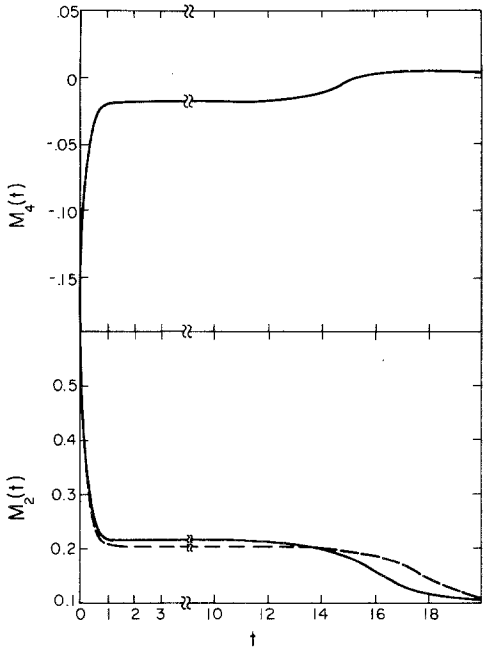


Fig. 8. $M_2(t)$ and $M_4(t)$ for the same conditions as Fig. 7. Note the break in the $t$ scale.

B $\rightarrow$ A evolution. The results for the D $\rightarrow$ C transition show the same qualitative features, except that the time evolution is slower by a factor of about three. In terms of the potential well picture, this slowing down can be understood from the fact that for states closer to the bifurcation point, the potential wells are shallower.

First consider $x(t)$ in Fig. 7. We also show the variation for the two approximations considered for the other two classes of initial conditions. The truncation $M_n = 0$, $n \geqslant 3$ yields, in this case, a slower approach to equilibrium as compared to Fig. 5; the successive truncations again show the straddling effect. The Nordholm–Zwanzig approximation for this situation leads to Eq. (34) as in case (i). This is also shown in Fig. 7 and again shows relatively rapid approach to equilibrium. The comparison of (exact) $x(t)$ and $M_3(t)$ shows that $M_3(t)$ reaches a minimum value around the time when $x(t)$ has climbed about halfway to its equilibrium value $x_0$. Equilibrium is reached by about $t = 25$; also, $x(t)$ and $M_3(t)$ do not change appreciably from their initial zero value for $t \leqslant 8$. The even cumulant moments $M_2(t)$ and $M_4(t)$ in Fig. 8 show the behavior, indicating distinct time stages during the approach to equilibrium. In the initial stage, both $M_2$ and $M_4$ show a rapid change. This is followed by a stage in which $M_2$ and $M_4$ maintain a

steady value; it is in the middle of this stage, roughly, that the odd moments pick up the pace of their time variation. In the final stage $M_2$ and $M_4$ again resume their further time variation to approach the equilibrium value. It is in this final stage that $M_3(t)$ overshoots its equilibrium value, goes through an extremum, and returns to the final equilibrium value.

The phenomena of a number of distinct time stages in the approach to a stable equilibrium from an initially unstable state of nonlinear systems has been noted recently by a number of authors.[4-7] A qualitative understanding of this phenomenon can be obtained by considering the behavior of $\rho(a, t)$ when initially it is placed (almost) symmetrically at the top of the central maximum in the double-well potential. Note first that ignoring $M_3$ and higher order cumulant moments does not alter the qualitative features of $x(t)$ and $M_2(t)$. Also, at the initial time $x(0)$ is almost zero and the half-width of the distribution $[\ln 2M_2(0)]^{1/2}$ is 0.624, whereas the expected final equilibrium values are 0.833 and 0.275, respectively; also, the intermediate steady value of $M_2$ corresponds to a distribution with a width of 0.382; initially, the wings of $\rho(a, 0)$ already envelop $\pm x_0$. Since $x(0)$ already is made to tip the distribution eventually towards the right well, $+x_0$, the system already has a slight asymmetry with respect to $x = 0$. For a very short time initially, the system seems to sharpen the distribution as a preparation for the eventual fall to the right well. Once this is achieved, the distribution starts to move to the right ever so slowly. Somewhere around $t \simeq 13$, the order parameter $x(t)$ has the value about 0.19, almost one-half of the current width of the intermediate stage distribution; most of the bell shape is now to the right—it is ready to fall into the well. This is the final stage, when the left half of the distribution may fall faster than the right half, thus creating further necessary sharpening of the distribution. The development of asymmetry of $\rho(a, \infty)$ through $M_3$, $M_5$, etc., can also be understood from the fact that the right (or left) well is not symmetric in steepness on two sides of the minimum.

From the SCDMF, Eq. (20), we have also studied the linear response of the system around the *stable* equilibrium (see cautionary remarks in Ref. 7 regarding the linear response around the unstable equilibrium state). We write

$$v(a_1) = v_0(a_1) + \theta[x(t) - x_0] \tag{36a}$$

$$\equiv -\{\partial U_0/\partial a_1 + \partial U_1/\partial a_1\} \tag{36b}$$

where

$$U_1(t) = -\theta[x(t) - x_0]a_1 \tag{37}$$

is to be viewed as the time-dependent perturbation. If we consider the system to be initially constrained in a local equilibrium with a specified value $x(0)$ for the order parameter,

$$\rho(a_1, 0) = Q_0^{-1} e^{-U_0/D}\{1 + \xi[x(0) - x_0]/\langle \xi^2 \rangle_0\} \tag{38a}$$

where

$$\xi = a_1 - x_0 \tag{38b}$$

and

$$\langle \xi^2 \rangle_0 = M_{20} \tag{38c}$$

then we can show that

$$[x(t) - x_0] = [x(0) - x_0]\psi_2(t) + \theta \int_0^t ds\, \chi(s)[x(t-s) - x_0] \tag{39a}$$

with

$$\psi_2(t) = \langle \xi \tilde{\xi}(t) \rangle_0 / \langle \xi^2 \rangle_0 \tag{39b}$$

and

$$\chi(t) = -\langle v_0(a_1)\tilde{\xi}(t) \rangle_0 / D \tag{39c}$$

Here $\langle \cdots \rangle_0$ is the average over the equilibrium distribution $Q_0^{-1} \exp[-U_0(a)/D]$, and the time evolution of $\tilde{\xi}(t)$ is governed by Eq. (20) with $x(t) = x_0$. If we denote $[x(t) - x_0)]$ as $\delta x(t)$ and its Laplace transform as $\delta\hat{x}(\epsilon)$, etc., then since Eq. (39a) implies

$$\delta\hat{x}(\epsilon) = \delta x(0)\hat{\psi}_2(\epsilon)/[1 - \theta\hat{\chi}(\epsilon)] \tag{40}$$

we anticipate a "critical slowing down" to manifest itself when $\hat{\chi}(\epsilon)$ is close to $1/\theta$. Further reduction of $\hat{\chi}(\epsilon)$ can be made,

$$\hat{\chi}(\epsilon) = [(\theta - 1 + 3x_0^2)M_{20}\hat{\psi}_2(\epsilon) + 3x_0 M_{30}\hat{\psi}_3(\epsilon) + (M_{40} + 3M_{20}^2)\hat{\psi}_4(\epsilon)]D^{-1} \tag{41a}$$

where

$$\psi_n(t) = \langle \xi^{n-1}\tilde{\xi}(t) \rangle_0 / \langle \xi^n \rangle_0 \tag{41b}$$

We shall discuss further aspects of this approach elsewhere; of course a similar analysis of the full FPE (5) can also be considered.

We have also considered the eigenvalue analysis of the SCDMF Eq. (20) to obtain the lowest nonzero eigenvalue $\lambda_0$. If $\delta x(t)$ in Eq. (36a) is small and ignored, the terms $\theta x_0$ in $v(a_1)$ will produce an extra linear term in $U_0$, which makes the potential well on the right (if $x_0 > 0$) more favorable. For this case $\lambda_0^{-1}$ would correspond to the "passage over the barrier" time scale, a problem first considered by Kramers.[7,15] If we write

$$\rho(a, t) \sim h(a)e^{-U_0/D}e^{-D\lambda t} \tag{42}$$

then after some analysis (essentially identical to that in Ref. 15), we get for the lowest nonzero eigenvalue ($\theta < 1$)

$$\lambda_0 = [(1 - \theta)/(\sqrt{2}\,\pi D)] \exp[-(1 - \theta)^2/4D] \tag{43}$$

which agrees with the result of Kramers, since the height of the barrier is $(1 - \theta)^2/4$.

## 5. SUMMARY

In this paper we have considered the equilibrium and dynamical behavior of a nonlinear stochastic model. The model consists of a large number of nonlinear oscillators, each oscillator interacting with all the others via a Weiss field. In the limit of weak nonlinearity, the model is analogous to the Ising–Weiss model. Even though the model does not contain spatial gradients, it does display a phase transition.

In equilibrium, the distribution $g_0(\mathbf{a})$ of the oscillator coordinates and the distribution $P_0(x)$ of the order parameter display non-Gaussian character, which originates from the nonlinearity. The non-Gaussian nature of $g_0(\mathbf{a})$ affects the value of the critical parameters $(\theta_c, D_c)$ significantly. For other properties also, the Gaussian approximation is quite inadequate near the transition point. (For this model, the transition point and the bifurcation point occur at the same position in the parameter space.)

We have used the cumulant expansion to study the approach to equilibrium for three different initial conditions. By using two different methods, we have obtained the same set of SCDMF equations [Eq. (22)] which the cumulant moments satisfy. The self-consistent dynamic mean field approach and, in particular, the ansatz in Eq. (19) could be applicable in many other nonlinear problems. For the initial nonequilibrium states considered in Section 4, the cumulant moment hierarchy has been rapidly convergent. The results display many interesting characteristics for the time evolution of cumulant moments. These are as follows:

1. If at $t = 0$, $x$ is altered by a large amount and higher order cumulant moments begin the time evolution with their equilibrium values, then these moments with $n > 1$ show a quick initial surge, indicating fluctuation enhancement, followed by a slow return to equilibrium values.

2. During the time evolution that takes the system from an initial unstable equilibrium to a final stable equilibrium, three distinct time stages are seen. In the initial stage, even moments show a rapid variation, while the odd moments retain their nearly zero values. In the intermediate stage, odd moments pick up the pace of their time variation, whereas the even moments go through a plateau and in the final stage, all the moments vary in time to reach their final equilibrium values.

3. For the simulation in which an initially ordered nonequilibrium state goes to an equilibrium disordered state, the order parameter as well as the higher order cumulant moments display a monotonic approach to equilibrium.

Many of these characteristics can be understood in qualitative terms (Section 4). These results may also provide fertile ground for testing some of the recent theoretical ideas[7,9] in the study of nonlinear systems.

## APPENDIX. CUMULANT MOMENT EQUATIONS

$$\dot{x} = (1 - x^2)x - 3xM_2 - M_3 \tag{A1}$$

$$\tfrac{1}{2}\dot{M}_2 = (1 - \theta - 3x^2)M_2 + \theta\mu_{12} - 3M_2{}^2 - 3xM_3 - M_4 + D + (\theta/N)(M_2 - \mu_{12}) \tag{A2}$$

$$\tfrac{1}{2}\dot{\mu}_{12} = (1 - 3x^2)\mu_{12} - 3M_2\mu_{12} - 3x\mu_{112} - \mu_{1112} + (\theta/N)(M_2 - \mu_{12}) \tag{A3}$$

$$\tfrac{1}{3}\dot{M}_3 = (1 - \theta - 3x^2)M_3 + \theta\mu_{112} - 9M_2M_3 - 3xM_4 - 6xM_2{}^2 + (\theta/N)(M_3 - \mu_{112}) \tag{A4}$$

$$\tfrac{1}{3}\dot{\mu}_{112} = (1 - \tfrac{2}{3}\theta - 3x^2 - 5M_2 - 2\mu_{12})\mu_{112} + \tfrac{2}{3}\theta\mu_{123} - 2\mu_{12}M_3 - x[2\mu_{1112} + \mu_{1122} + 4M_2\mu_{12} + 2(\mu_{12})^2] + (\theta/3N)(3\mu_{112} + M_3 - 4\mu_{123}) \tag{A5}$$

$$\tfrac{1}{3}\dot{\mu}_{123} = (1 - 3x^2 - 3M_2)\mu_{123} - 6\mu_{12}\mu_{112} - 3x[\mu_{1123} + 2(\mu_{12})^2] + (2\theta/N)(\mu_{112} - \mu_{123}) \tag{A6}$$

$$\tfrac{1}{4}\dot{M}_4 = (1 - \theta - 3x^2)M_4 - 18xM_2M_3 - 12M_2M_4 - 6(M_2)^3 - 9(M_3)^2 + \theta\mu_{1112} + (\theta/N)(M_4 - \mu_{1112}) \tag{A7}$$

$$\tfrac{1}{4}\dot{\mu}_{1112} = (1 - \tfrac{3}{4}\theta - 3x^2 - \tfrac{15}{2}M_2)\mu_{1112} + \tfrac{3}{4}\theta\mu_{1123} - 9x[M_2\mu_{112} + \tfrac{1}{2}\mu_{12}(M_3 + \mu_{112})] - \tfrac{3}{2}[\mu_{12}(\tfrac{3}{4}M_4 + \tfrac{3}{2}\mu_{1122} + 3M_2{}^2 + \mu_{12}^2) + \tfrac{3}{2}\mu_{112}(3M_3 + \mu_{112})] + (\theta/4N)(M_4 + 2\mu_{1112} + 3\mu_{1122} - 6\mu_{1123}) \tag{A8}$$

$$\tfrac{1}{4}\dot{\mu}_{1122} = (1 - \theta - 3x^2 - 6M_2)\mu_{1122} + \theta\mu_{1123} - 6x\mu_{112}(M_2 + 2\mu_{12}) - 3(2\mu_{12}\mu_{1112} + 2M_2\mu_{12}^2 + 2\mu_{112}^2 + M_3\mu_{112}) + (\theta/N)(\mu_{1122} + \mu_{1112} - 2\mu_{1123}) \tag{A9}$$

$$\tfrac{1}{4}\dot{\mu}_{1123} = (1 - \tfrac{1}{2}\theta - 3x^2 - 3\mu_{12} - \tfrac{9}{2}M_2)\mu_{1123} + \tfrac{1}{2}\theta\mu_{1234} - 3x[2\mu_{12}\mu_{112} + \mu_{123}(\mu_{12} + M_2)] - \tfrac{3}{2}[2(M_2 + \mu_{12})\mu_{12}^2 + 3\mu_{112}^2 + (M_3 + 2\mu_{112})\mu_{123} + (2\mu_{1112} + \mu_{1122})\mu_{12}] + (\theta/2N)(\mu_{1112} + \mu_{1122} + \mu_{1123} - 3\mu_{1234}) \tag{A10}$$

$$\tfrac{1}{4}\dot{\mu}_{1234} = (1 - 3x^2 - 3M_2)\mu_{1234} - 18x\mu_{12}\mu_{123} - 3(2\mu_{12}^3 + 3\mu_{112}\mu_{123} + 3\mu_{12}\mu_{1123}) + (3\theta/N)(\mu_{1123} - \mu_{1234}) \tag{A11}$$

## ACKNOWLEDGMENTS

A large portion of this work was done in 1975 during our sabbatical leave at the California Institute of Technology. We would like to thank Prof. C. J. Pings and Prof. N. Corngold for their hospitality. One of us (RCD) would also like to thank Dr. W. H. Enright and Dr. I. Farkas for useful discussions on stiff nonlinear differential equations.

## REFERENCES

1. Z. A. Akcasu, *J. Stat. Phys.* **16**:33 (1977).
2. R. Kubo, K. Matsuo, and K. Kitahara, *J. Stat. Phys.* **9**:51 (1973).
3. R. Zwanzig, *Phys. Rev.* **124**:983 (1961).
4. R. Zwanzig, in *Statistical Mechanics, New Concepts, New Problems, New Applications*, S. A. Rice, K. F. Freed, and J. C. Light, eds. (University of Chicago Press, Chicago, Illinois, 1972), p. 241.
5. R. Zwanzig, K. S. J. Nordholm, and W. C. Mitchell, *Phys. Rev. A* **5**:2680 (1972).
6. K. S. J. Nordholm and R. Zwanzig, *J. Stat. Phys.* **11**:143 (1974).
7. N. G. Van Kampen, *J. Stat. Phys.* **17**:71 (1977).
8. N. G. Van Kampen, *Can. J. Phys.* **39**:551 (1961).
9. M. Suzuki, *J. Stat. Phys.* **16**:11 (1977), and references therein.
10. K. Kometani and H. Shimizu, *J. Stat. Phys.* **13**:473 (1975).
11. M. Kac, in *Statistical Physics, Phase Transitions and Superfluidity*, M. Chre'tien, E. P. Gross, and S. Deser, eds. (Gordon and Breach, 1968), Vol. 1, p. 241.
12. M. Abramowitz and I. A. Stegun, eds., *Handbook of Mathematical Functions* (Dover, 1965), Sec. 19.3, p. 687.
13. Y. Onodera, *Prog. Theor. Phys.* **44**:1477 (1970).
14. W. H. Enright, *SIAM J. Numer. Anal.* **11**:321 (1974), and references cited therein.
15. S. Chandrasekhar, *Rev. Mod. Phys.* **15**:1 (1943), Ch. III, Sec. 7.